

TOPOLOGICAL OPTIMISATION OF LARGE, ADDITIVELY MANUFACTURED COMPOSITE STRUCTURES WITH A GRADED LATTICE CORE

A. Moss¹, T. Macquart², A. Panesar³, P. Greaves⁴, M. Forrest⁵, A. Pirrera⁶

¹ PhD Candidate, Bristol Composites Institute, Queen's Building, University of Bristol, Bristol, BS8 1TR, UK, alex.moss@bristol.ac.uk, https://www.researchgate.net/profile/Alex_Moss13

² Lecturer in Aeroelastics, Bristol Composites Institute, Queen's Building, University of Bristol, Bristol, BS8 1TR, UK, terence.macquart@bristol.ac.uk, <https://research-information.bris.ac.uk/en/persons/terence-macquart>

³ Senior Lecturer (Associate Professor), Department of Aeronautics, City and Guilds Building, Imperial College London, London, SW7 9AG, UK, a.panesar@imperial.ac.uk, <https://www.imperial.ac.uk/people/a.panesar>

⁴ Principle Research Engineer, Blade Structures, Offshore Renewable Energy Catapult, Offshore House, Blyth, NE24 1LZ, UK, peter.greaves@ore.catapult.org.uk, <https://ore.catapult.org.uk/people/peter-greaves/>

⁵ Blade Research Leader, Offshore Renewable Energy Catapult, Offshore House, Blyth, NE24 1LZ, UK, mark.forrest@ore.catapult.org.uk, <https://ore.catapult.org.uk/people/dr-mark-forrest/>

⁶ Professor of Nonlinear Structural Mechanics, Bristol Composites Institute, Queen's Building, University of Bristol, Bristol, BS8 1TR, UK, alberto.pirrera@bristol.ac.uk, <https://research-information.bris.ac.uk/en/persons/alberto-pirrera>

Keywords: Topology optimisation, Additive manufacturing, Cellular architectures, Lattice Cores, Composite structural design

ABSTRACT

Interest in the use of additive manufacturing has grown within many engineering sectors. A notable application is that of low density core structures, utilising repeated unit cell graded lattices to enable improved efficiency and manufacturability. Used in combination, composite laminates and 3D printed graded lattices can achieve the high specific strength and stiffness required for large-scale structures such as wind turbine blades.

In this study, a novel methodology based on topology optimisation for additive manufacturing was applied to the design of two composite-graded lattice-hybrid structures. The novel methodology involves a multi-step topology optimisation process which first generates composite laminate designs based on the main load paths and then finds the optimal distribution of 3D printed material in the form of self-supporting graded lattices. This work aims to create initial design points for this methodology through idealised load cases so that simple comparisons can be drawn between designs produced through topology optimisation and conventional solutions such as composite beams and sandwich panels.

It was found that there are significant performance differences between the idealised graded density field and the optimised graded lattice geometry. This is shown to be affected by the input parameters to the optimisation and by the choice of unit cell size in the lattice. The composite laminate sizing process is shown to produce structurally feasible and manufacturable solutions, showing that the design can be tailored for mass and cost. This work indicates that the novel design methodology can potentially produce improvements in performance over traditional sandwich composite structures.

1 INTRODUCTION

Additive manufacturing (AM), commonly known as 3D printing, is increasingly gaining prominence in structurally demanding applications across many engineering sectors [1]. This is attributed to its capacity to produce intricate shapes with complex internal geometry, such as the cellular architectures shown in Figure 1, unattainable through traditional manufacturing methods. These cellular lattices help to reduce weight and improve structural performance.

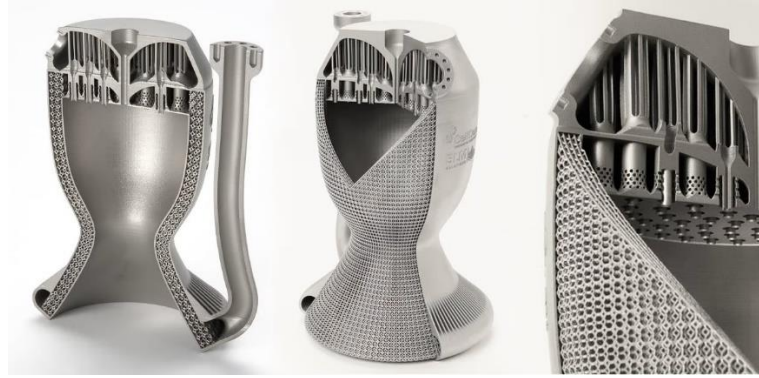


Figure 1: 3D printed single-piece rocket propulsion engine. [2]

The interest in lattice structures as a replacement for conventional foam and honeycomb cores is largely due to their potential for high efficiency and multifunctionality [3–4]. 3D printed graded lattice structures have demonstrated improved structural performance in both static and dynamic applications, providing higher overall stiffness and energy absorption than homogeneous lattices of the same weight [5–6]. This high structural efficiency is enabled through density-based topology optimisation (TO), where the distribution of material within a design region is varied to maximise a specific performance indicator such as stiffness [7]. The design produced from topology optimisation is then realised through the 3D printing of graded lattices.

For large-scale structures such as wind turbine blades, 3D printed components cannot compete with conventional composite laminates in terms of specific strength and stiffness. For beam and panel structures, the efficiency of composites is unparalleled due to the highly directional properties of the fibre reinforcement. However, the advantages of printed lattices can be realised through full utilisation of the three dimensions of space, efficiently distributing low density material. For a wind blade, much of the internal void space could be utilised, with graded lattices supporting the composite laminate panels. This combination of laminated composites and lattices has already been demonstrated in highly efficient sandwich structures [8], enabling improved structural performance with components which are readily manufacturable.

To design such composite structures, the author has previously proposed a novel multi-step topology optimisation framework [9]. This can be summarised by three of its main stages, shown in Figure 2;

- 1) A topology optimisation is conducted on a given geometry and load case to size composite laminates based on the location and shape of the full density features (e.g. load path) in the solution.
- 2) With the laminates sized and frozen, a second topology optimisation is conducted to find the best lattice configuration to support and connect the laminated regions.
- 3) The topologically optimised density field from (2) is then mapped onto an equivalent graded lattice.

There are two unknowns in the proposed design process which must be investigated, the laminate sizing and the graded lattice conversion. Topology optimisation, especially solid isotropic material and penalisation (SIMP) is well documented as being capable of producing the best theoretical isotropic solutions [10]. For the design of fibre-reinforced composite structures, there are many limitations to the applicability of more advanced methods of topology optimisation [11]. Overcoming these limitations is deemed outside the scope of the present work. Nevertheless, the distribution of material from SIMP topology optimisation can be assumed to show the load paths and therefore primary stiffness directions.

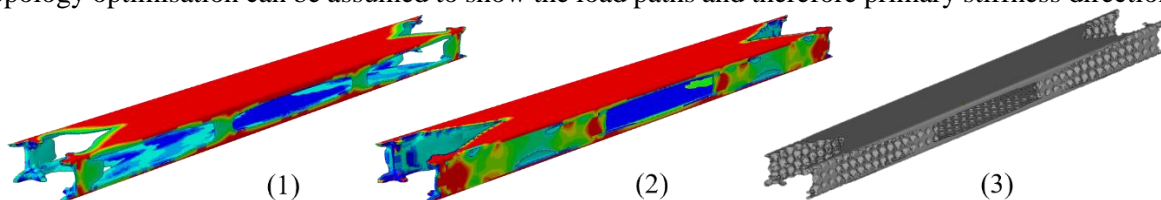


Figure 2: Multi-step topology optimisation process applied to a box beam geometry.

Thereafter, converting a load path from topology optimisation into a laminated component will require engineering judgment. Therefore, this step in the proposed design methodology requires investigation. The primary concern being the production of a laminate design that is both realistic and manufacturable, while still maintaining similarity to the first TO solution to retain the desired performance. In other words, the discrepancy between the response of the original TO solution and the laminated adaptation should be minimised.

Similar scrutiny needs to be placed on step 3 of the design methodology. In order to address the potential mismatch of the conversion from optimised density field to graded lattice, printing capabilities must be considered. Most commercial 3D printers have a nozzle size of 0.4 mm, which therefore restricts the minimum wall thickness of the unit cell. This defines the smallest realistically manufacturable unit cell, roughly 10 mm in edge length. It cannot be assumed that this unit cell size will capture the behaviour of the cellular lattice accurately, therefore the effect of this conversion process on the resulting structural properties of the final design configuration must be studied.

To understand the extent of the inaccuracy potentially caused by the conversion of topology optimisation solutions to realistic composite-graded lattice-hybrid structures, two representative design cases are proposed herein. The first case aims to identify the differences between the optimised density field and the optimised graded lattice by using a short beam configuration for shear-dominated behaviour. As the lattice structures will be used to transfer load between the laminates, they will primarily be under shear loading. Investigating the behaviour of the graded lattice cores focusing on shear deformation will be the most representative factor for structural performance. The shear deformation can be further isolated by adding two fixed thickness composite skins to resist the bending stress in a four-point bending load case.

The second case aims to verify the accuracy of the composite laminate sizing process through an optimisation of a longer beam ($L/t > 10$). This geometry change will enforce bending dominated loading in the structure. As our primary interest are wind turbine blades, this is an ideal case as it is likely to form 'spar cap'-type features in the solution. This shape will simplify the laminate sizing process and help to identify the best input parameters to use. If there are any differences between the performance of the first stage topology optimisation solution, the input to the second stage and the final result from stage 3, this will provide information about to what extent the graded lattice is helping to support the composite laminate structure.

This work aims to demonstrate this design process using idealised representative structures, to enable benchmarking analysis of the parameters for the topology optimisation and conversion processes. The proposed multi-step design methodology can then use this information to demonstrate an applied proof of concept, such as a wind turbine blade design. The simplistic nature of the representative geometries and load cases enables further validation of the results through experimental testing in future. In the following section, the short beam study is discussed first as it is the simpler of the two cases, due to its focus on the graded lattice design only.

2 BENCHMARK STUDY OF LATTICE STRUCTURAL DESIGN – SHORT BEAM

2.1 Methodology

The four-point bend test is a common testing configuration used to determine the flexural stiffness and strength of a material such as fibre composite. It is a versatile testing configuration, as multiple stress states are induced in the specimen. These include tension, compression, and shear from the bending action, as well as local compression stresses near the load introduction (roller) area. The size of the different stresses in the specimen can be adjusted by varying the sample dimensions. This versatility alongside the simplicity of the load application method makes a four-point bend test a good candidate for benchmarking the proposed topology optimisation design framework.

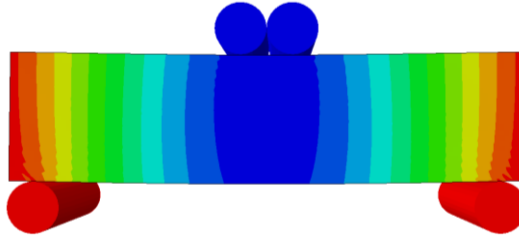


Figure 3: Loading configuration for which the short beam ($100 \times 50 \times 200$ mm) will be optimised.

The short beam size of $100 \times 50 \times 200$ mm was chosen so that the structure was shear dominated while still being long enough to justify the inclusion of a composite skin to resist bending. The presence of a composite skin is deemed necessary for consistency as representative of the type of composite-graded-lattice-hybrid structure that the proposed design methodology is meant to produce when applied to real structures like a wind turbine blade. In this study, the composite skin is taking the bending stresses allowing load separation. This means that the lattice structure optimisation is primarily resisting the shear and roller compression stresses. This will help to identify the differences in performance between the optimised density field and the graded lattice in an ideal use case. The unidirectional composite skin chosen was IM7/8552 using the material properties from [12]. The properties applied to the skin and core region are shown in Table 1.

Material	Primary Stiffness (GPa)	Transverse Stiffness (GPa)	Poisson Ratio	Shear Stiffness (GPa)
UD Carbon	161	11.7	0.32	5.17
Core	2.6	~	0.3	~

Table 1: Material properties used in the Abaqus model.

For the short beam structure, the middle rollers of the four-point-bend case will be moved close together, as shown in Figure 3, to increase the maximum bending moment as failure in the skin will not occur with such a short beam. This also increases the amount of local compression in the mid region as the loads interact, making a pseudo-three-point-bend load case. This is useful as it increases the contribution of maximum direct compression, more in line with the shear loading contribution, so that the effect of both loading types can be studied.

To speed up the analysis, a quarter model is used by applying symmetric boundary conditions. This is only possible because of the symmetry of the load case. Additionally, to make the resulting structural design symmetric in the Y direction, two opposite four-point bend load cases are applied to the model in the TO phase. These load cases are designed to induce symmetric loading conditions on the beam. This is also a simple way to benchmark the effect of multiple competing load cases on the proposed design method.

The TO algorithm of Abaqus [13], our software of choice, does not work with contact interactions. However, the contact pressures can be approximated using a constant pressure field. To model the boundary conditions, the vertical motion can be prevented just like the roller would in the four-point-bend rig. By applying appropriate constraints of zero vertical displacement along a node region, the fixed roller boundary condition can be assumed to be enforced. The accuracy of this approximation can be tested before and after the optimisation process, on the solid short beam and the optimised short beam, by conducting analysis with both the contact interactions and the approximations.

To model the behaviour of the lattice-laminate interface, it is assumed that the UD laminate is a skin on top of a flat solid sheet of PLA, which the lattice is connected to. This would result in the best possible adhesion between the PLA and laminate, meaning that we assume there will be no de-bonding. To ensure this solid PLA region is modelled correctly in the optimisation, a 1 mm region at the top and bottom of

the beam is frozen. The skin is then defined on these solid PLA surfaces. There are many parameters required for TO in Abaqus, these are shown in Table 2 and the choice for the key factors is elucidated below.

Parameter	Setting
<i>Objective Function</i>	Minimise Volume
<i>Constraint</i>	Mid-point Displacement
<i>Constrain Value</i>	1.1 mm
<i>Penalisation Factor</i>	1
<i>Soft Element Method</i>	Standard
<i>Soft Element Threshold</i>	0.15
<i>Density Update Strategy</i>	Conservative
<i>Initial Density</i>	0.3
<i>Maximum Density Move</i>	0.01
<i>Mesh Seed Size</i>	2 mm
<i>Minimum Feature Size</i>	6 mm

Table 2: Abaqus Topology Optimisation Parameters.

Modelling the density-stiffness relationship of the graded lattice involves the use of a penalisation factor, a power-law relationship which reduces the efficiency of intermediate densities. When using higher penalisation factors in the topology optimisation, the features in the solution tend towards truss structures. These features are not readily manufacturable using lattice or laminate structures and tend to be more associated with the 3D printing of solid-void topology optimisation designs. For this study, the intermediate densities are not penalised, as this gives the best possible chance at a global minimum solution and produces ‘greyscale’ solutions which can only be realised using graded lattices.

The feature minimum radius value (RMIN) is set at 150% of the mesh size so that checkerboarding is prevented. A higher RMIN value would be ‘smoothing’ the density distribution, not allowing rapid change of density from solid to void where it is most important for the optimality of the solution. It is possible to begin to remove low density elements from the analysis within the optimisation by using a strategy which Abaqus defines as ‘soft elements’. In this method, any element which is below a certain density threshold and is surrounded by elements also below this threshold value can be removed from the analysis without invalidating the mesh. In this way, manufacturing and modelling constraints on the unit cells of the lattice can be imposed in the optimisation, meaning that any regions of low density which would be removed by the latticing process, i.e. the process that converts a density field into a graded lattice, do not cause differences in the resulting performance.

In the previous work outlining the design methodology for a wind blade [9], the input for the topology optimisation used was the optimal displacement values for maximum power output. For our representative geometries, there is no previous analysis to provide these optimal displacement values, therefore they were produced using a conventional minimum compliance topology optimisation. This optimisation result is ideal as it is a known feasible solution to this design case. This minimum compliance topology optimisation would result in an ‘optimal’ midpoint displacement, which is then used as the target absolute displacement for a minimise volume optimisation.

Once the optimised density field is generated, it is used as an input for LatTess [14], which generates a graded lattice geometry closely matching the density distribution of the topology optimisation solution. LatTess uses grading within and between unit cells to better agree with the density field, improving accuracy. A range of different triply period minimal surfaces (TPMS) unit cells are available, but the ‘primitive’ is chosen due to its theoretically superior manufacturability over other TPMS and truss-based lattices. This geometry is then output as an STL file for further modelling or manufacturing.

An important input parameter for LatTess is unit cell edge length. The best edge lengths for the short beam were 10 mm, 12.5 mm and 25 mm. These were chosen for two reasons: 1. The unit cells must be 10 mm or larger and the beam must be more than 1 unit cell high; 2. Each of the beam dimensions can be divided by them without remainder, making modelling easier; 12.5 mm was chosen for the baseline result as it is in the middle. Designs with 10 mm and 25 mm edge lengths will be modelled additionally to investigate the effect of varying the unit cell size on the displacement performance.

2.2 Results

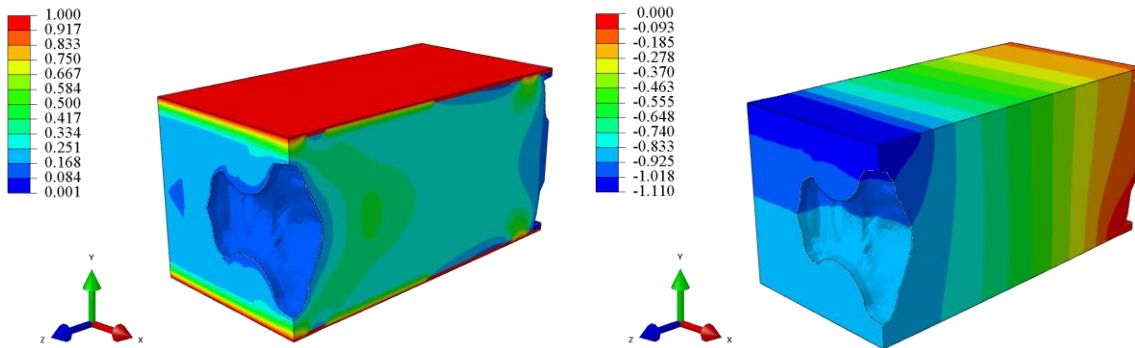


Figure 4: Quarter model result for short beam optimisation (a) Density (b) Displacement.

Initial results for the short beam design process are shown in Figure 4. In this optimisation result, basic features of shear load transfer can be seen, with diagonal regions of $\sim 50\%$ volume fraction and large regions of low density sharing the load. This efficiently uses material of a range of densities to support and connect the stiff composite laminates. Void regions form where there is no load transfer, which occurs as the shear load path travels diagonally between the upper and lower ‘roller’ application points.

Figure 5 shows the graded lattice, which matches the density distribution from Figure 4a, under the design load case. This result indicates that the displacement when using the graded lattice geometry is double that of the optimised density field result shown in Figure 4b. There are several possible reasons for this, the most likely being that the penalisation factor chosen drastically overestimates the stiffness of the lattice core. Other possibilities include geometrical defects from the lattice conversion process, such as is shown in Figure 6.

To rule out the effect of these discontinuities on the lattice performance, another topology optimisation was conducted with the minimum relative density set to 0.15. This would prevent any discontinuities in the lattice walls while not drastically changing the performance, as the initial solution had few void regions. The updated topology optimisation solution is shown in Figure 7.

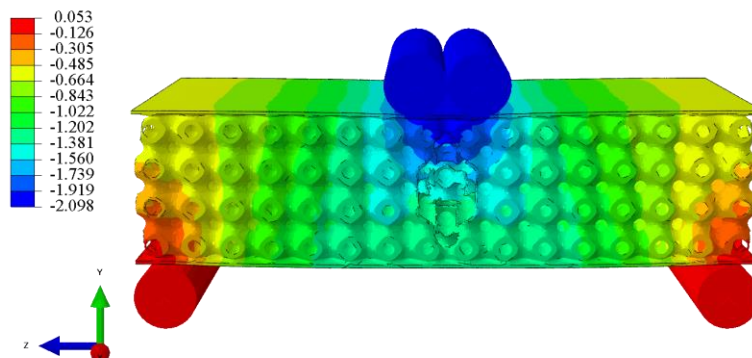


Figure 5: Full graded lattice composite model under four-point bending rig – Displacement.

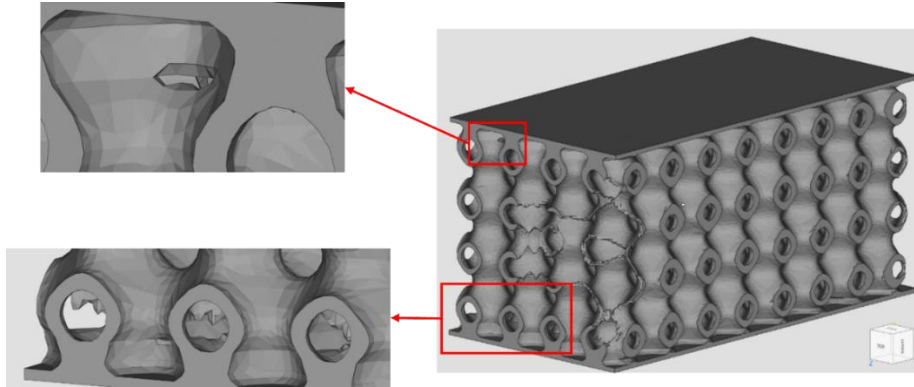


Figure 6: STL visualisation of optimised graded lattice, showing the presence of small discontinuities.

The updated composite graded lattice designs were subjected both the pressure load approximate and contact interaction loading cases to identify discrepancies in the displacement distributions, shown in Figure 8. There is reasonable agreement in average midpoint displacement, but Figure 8a shows a varying displacement distribution across the X direction. This difference will need to be studied in more detail, so that the composite structures are designed using a more accurate approximation of roller contact forces. This will improve the level of agreement with future results from experimental validation.

The displacement at the midpoint is still almost double that of the imposed constraint in the optimisation, indicating that it is not the discontinuities in the lattice wall causing a reduction in stiffness in the short beam. They may have slightly improved performance by having continuous surfaces through which load can transfer unimpeded, but this effect was clearly negligible. The contrast in displacement between the optimised density field and the graded lattice is dominated by the crushing effect of the roller force. The crushing effect can be measured by taking the difference between the top and bottom of the midpoint of the beam. In the optimised density field result this difference is 0.15 mm, but in the graded lattice result

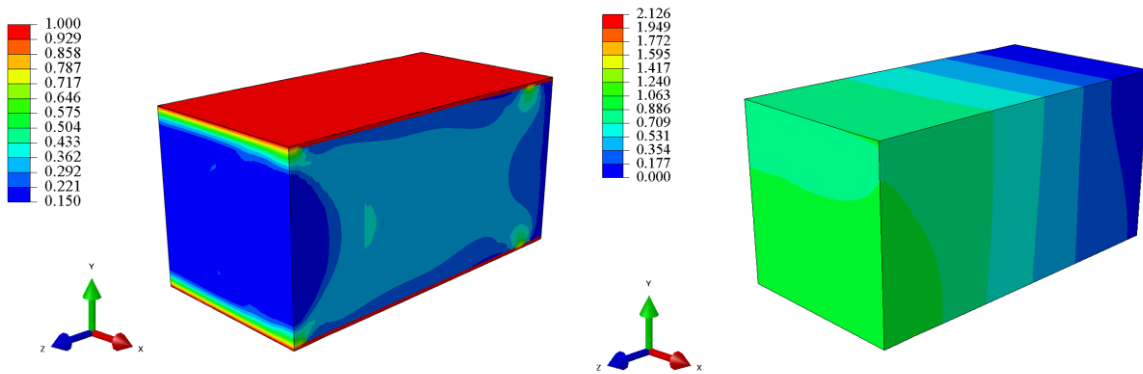


Figure 7: Updated short beam optimisation result (a) Relative density (b) Displacement.

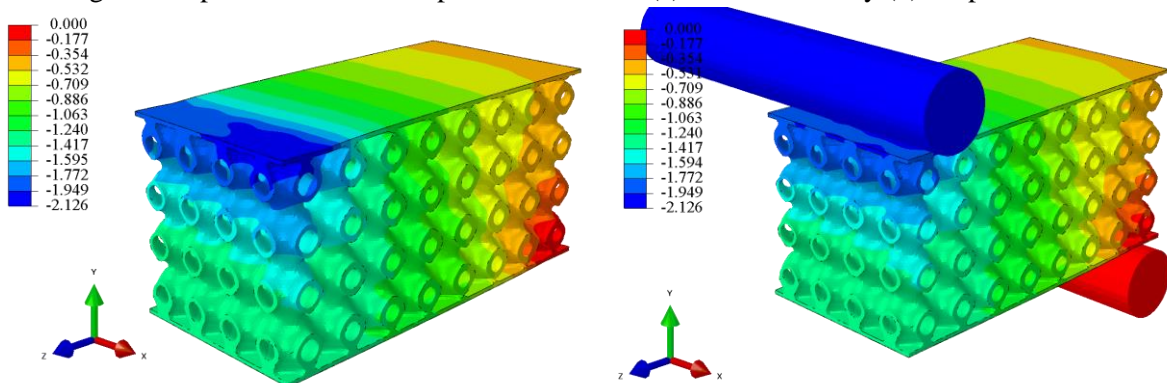


Figure 8: Graded lattice with 12.5 mm unit cell edge lengths under loading. (a) Approximate roller boundary conditions applied. (b) Contact interactions with rollers applied.

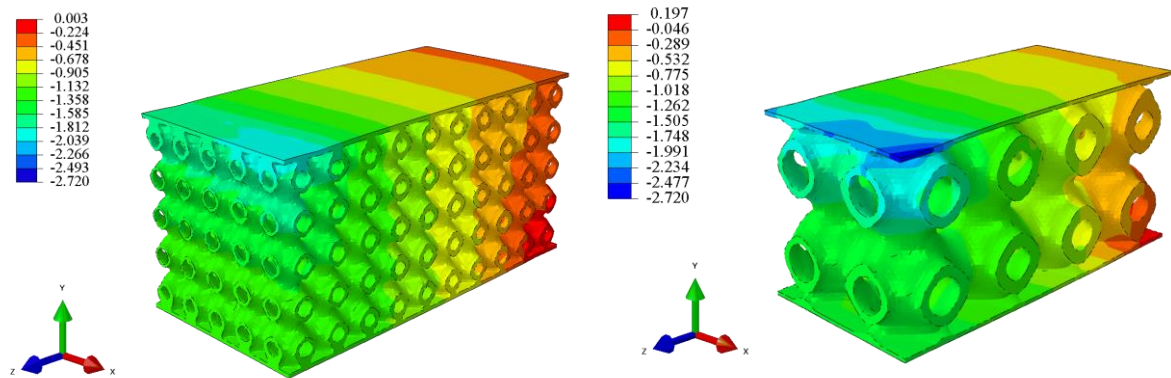


Figure 9: Graded lattice beam results (a) 10mm unit cell edge length (b) 25mm unit cell edge length.

it is 0.55 mm, almost 4 times larger. This indicates a mismatch between the assumed direct compressive stiffness of the lattice region in the optimisation and the graded lattice geometry. Intuitively, it follows that the mismatch in shear stiffness is also significant, even if it is less than for the direct compressive stiffness. By ruling out all other causes, it is shown that penalising the intermediate densities negatively impacts the performance of the graded lattice and the design process as a whole.

The effect of the unit cell size was investigated by varying the characteristic edge length of the cell. As the grading method allows for the same density field to be mapped to lattices with different cell sizes, the size effect can be measured. The results for the 10 mm and 25 mm unit cell lattices are shown in Figure 9. The 10 mm unit cell shows lower displacement, indicating improved performance as the unit cell size is decreased. The 25 mm result supports this trend, showing higher displacement and therefore worse performance. The 25 mm result also shows that the roller load approximation fails to mimic the roller contact pressure for larger unit cells, as the constant pressure applies a bending force to the thin panel between unit cell walls where it is not supported from below. This results in higher displacement values than would occur in a roller contact interaction analysis.

The extent to which the unit cell size affects the mass through the latticing process is not known, but the volumes from the optimised density fields can be used to estimate this value. At just under 400 g, this is on the heavy side for a composite structure. For example, aerospace grade ROHACELL[®] HERO 200 foam used in place of the lattice in this design would reduce the mass by roughly 150 g. With improvements in the design process through the correct choice of parameters, the lattice may be able to compete with aerospace grade foam in specific stiffness. This load case is however not representative of how the graded lattices will be used in composite design, as there is no need for 3D printed parts to resist any of the primary loads. This is the remit of the first stage of the topology optimisation design process, leaving the lattices to provide improved manufacturability as well as structural support for complex multi-directional load paths.

3 BENCHMARK STUDY OF LAMINATE DESIGN – LONG BEAM

3.1 Methodology

The long beam size of $100 \times 50 \times 600$ mm was chosen so that the structure would deform primarily in bending, therefore the resulting optimisation would generate solid regions in the solution which resemble composite spar caps. This is an ideal case for studying the laminate sizing aspect (1) of the design methodology, as the features generated will be thin enough to assume limited through thickness load transfer. In the first stage optimisation, a quasi-isotropic laminate stiffness is applied as a fully isotropic material property, to enable the optimisation to find the main load paths unrestricted and unbiased. With this information, an assumption can be made that the load paths are directional, and a ‘thin laminate’ feature demonstrates limited through thickness load transfer.

As the method of loading in the optimisation, mimicking roller forces, has been demonstrated previously, this will again be used for this geometry. The only change is to move the middle rollers apart to make a true four-point bending load case, so that the beam is split into bending moment only and mixed loading type regions. This means that features in the optimisation will vary between regions, making them more easily identifiable. A quarter model will again be used with the two symmetric load cases to maintain a triply symmetric design.

As with the previous study, the displacement constraints will be generated by first conducting a minimum compliance topology optimisation with a volume constraint, to ensure that the topology optimisation design is targeting a known ‘optimal’ midpoint displacement value. The parameters for this first stage topology optimisation are shown in Table 3. In the first stage optimisation, similar to the short beam study, a penalisation factor of 1 and an RMIN of 150% of the mesh size was used. The soft element strategy was not used, as it would add additional constraints to the optimisation and largely only affects the low-density regions, which do not impact the laminate sizing process.

The laminate sizing process involves post-processing the first stage solution to identify elements above and below a density threshold value. An example using 50% relative density as the threshold is shown in Figure 12. A one element thick region at the top and bottom of the model is also made solid to include continuous support between the solid region of the spar cap and the roller support near the end. This strategy was chosen to maintain material continuity between the fixed rollers, to ensure similarity with the short beam study and to include the high density regions which form at the fixed rollers, shown in Figure 11. These solid laminate regions are given unidirectional carbon fibre composite properties, upgrading them from quasi-isotropic properties. This is done as even the lower density regions of the first stage solution are still much stiffer than PLA, even 5% of the isotropic stiffness in the first stage is higher than solid PLA. The upgraded stiffness is required for the second stage optimisation to meet the displacement constraints imposed.

A study will be conducted where the density threshold value is varied to produce multiple second stage optimisation designs with different laminate and lattice configurations. The mass of these designs will be compared to identify the optimal parameter to use in the laminate sizing process. As this laminate sizing process will focus on the bending resistant features of the beam, this again isolates the lattice optimisation stage in its goal to provide structural support and connectivity to the composite. The lattice design will primarily target shear load transfer between ‘spar caps’ and locally high crushing forces near the roller contacts. The second stage optimisation will be identical to the short beam process, freezing the laminate region and optimising only the lattice, using the soft element strategy to improve agreement between density field and lattice performance.

Parameter	Setting
<i>Objective Function</i>	Minimise Volume
<i>Constraint</i>	Mid-point Displacement
<i>Constraint Value</i>	2mm
<i>Penalisation Factor</i>	1
<i>Soft Element Method</i>	None
<i>Soft Element Threshold</i>	0
<i>Density Update Strategy</i>	Conservative
<i>Initial Density</i>	0.3
<i>Maximum Density Move</i>	0.01
<i>Mesh Seed Size</i>	2
<i>Minimum Feature Size</i>	6

Table 3: Abaqus Topology Optimisation Parameters.

3.2 Results

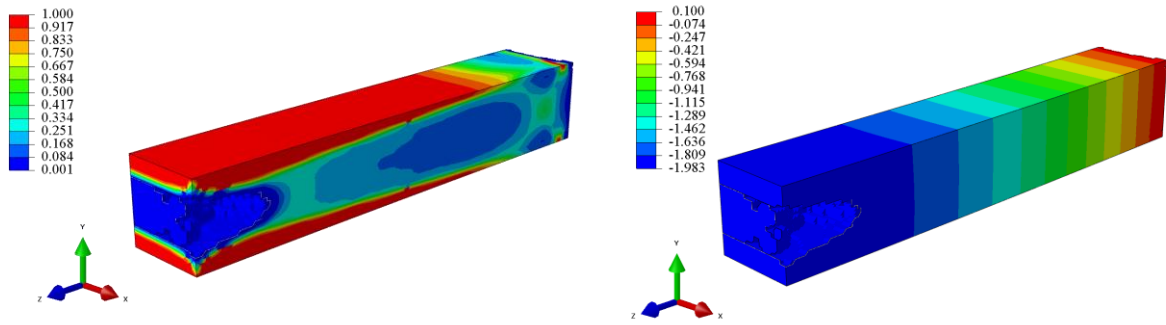


Figure 11: First stage topology optimisation solution (a) Relative density (b) Displacement.

The first stage of optimisation is shown in Figure 11. The choice of geometry has guided the optimisation towards the design which was expected. The main features of the design are the two solid regions which can be referred to as ‘spar caps’, which are relatively simple to convert to laminate geometry due to the similarity to a wide, flat plate. This is because the geometry of the optimised configuration is driven by a principal stiffness direction, in this case it is longitudinal stiffness used to improve bending rigidity. This means a straight swap for unidirectional carbon fibre will make minimal changes to the optimality in the transverse directions but is highly efficient in the primary stiffness direction. Subsidiary load paths within the solution will generally not be as easily translated into features commonly associated with composite structural design such as shear webs and cylinders. The pillar at the middle roller location is not suitable for unidirectional composite as it is under compression and shear loading in this design.

Figure 12 shows where unidirectional carbon laminate properties have been assigned, forming conventional laminate shapes which could be manufactured. 3D orthotropic properties, shown in Table 5, are used for the unidirectional carbon laminate. The lattice core full density property from Table 1 is used again in the second stage optimisation.

E11	E22	E33	ν_{12}	ν_{13}	ν_{23}	G12	G13	G23
161	11.7	11.7	0.32	0.32	0.45	5.17	5.17	3.98

Table 5: Orthotropic material properties for solid composite elements (GPa)

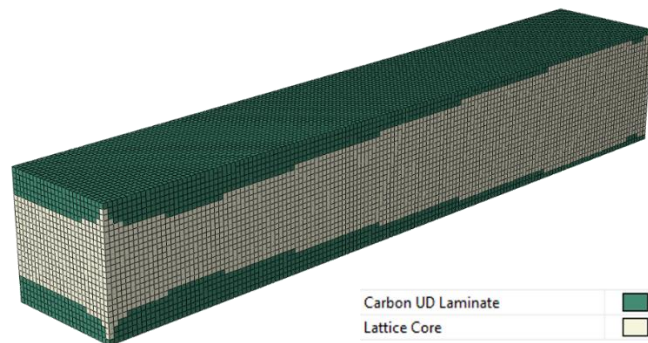


Figure 12: Breakdown of applied section properties for second stage optimisation with laminate sized using a relative density threshold value of 0.5.

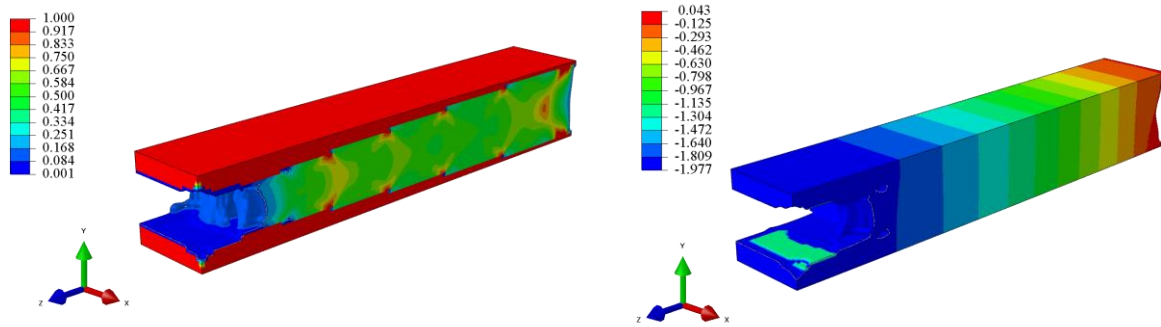


Figure 13: Second stage topology optimisation solution using a relative density threshold of 0.5 for the laminate sizing (a) Relative density (b) Displacement.

Figure 13a shows that the core generated in stage 2 of the design methodology supports the laminates in shear with low density regions across the whole domain, with distinct variations where the load varies such as in the middle where there is no shear load transfer required, as well as locally building up the density near ‘ply-drops’. Also present at these ply-drop locations are individual elements with low density which would result in small holes in the geometry if allowed to remain during the latticing process. This demonstrates the need for a patch to the latticing process and future study into the effect of locally increasing densities to improve manufacturability and structural performance.

The effect of varying the density threshold parameter in the laminate sizing on the mass of the final configuration is shown in Figure 14. The trend shows that, as the density threshold reduces from 1, the mass of the final configuration decreases. The reducing core volume fraction is an indicator of why this is happening, because the increased amount of laminate material from lowering the threshold means that the design is stiffer, therefore less core material is needed to support the laminate in meeting the displacement constraints. On top of this, as the laminate volume increases, the lattice core optimisation domain volume decreases, because the total volume of the design space remains the same. This is why moving the threshold from 1 to 0.5 only decreases the mass by 2.4%, because the decrease in lattice core volume is almost matched by increase in laminate volume. This shows that a trade-off can be made in this design process between mass and cost, as more composite laminate will provide an improved design but the material cost would be higher because PLA is cheaper than carbon fibre.

At the lower end of the density threshold scale, it seems as if the design is far superior. This sharp drop off in mass is explained by the appearance of features in the solution which are unrealistic and not manufacturable. As the threshold value goes below 0.5, the laminate sizing begins to include elements which invalidate the assumption of manufacturability, e.g. the pillar support at the middle roller location.

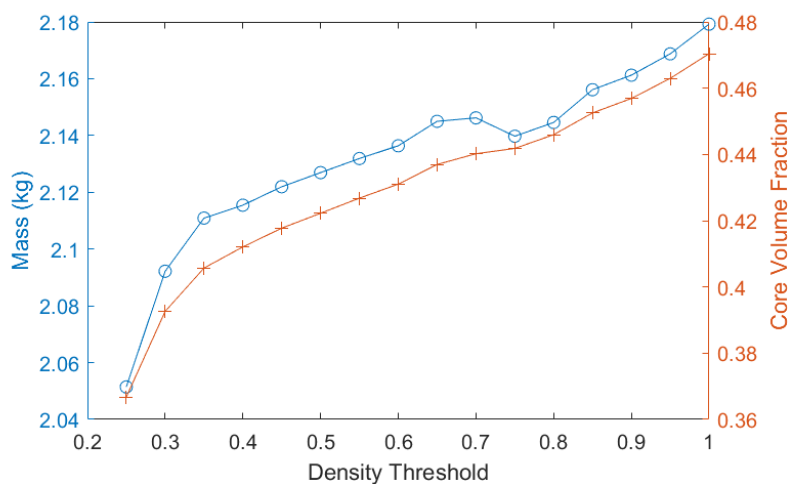


Figure 14: Effect of varying the laminate sizing relative density parameter on the mass and core volume fraction of the final design.

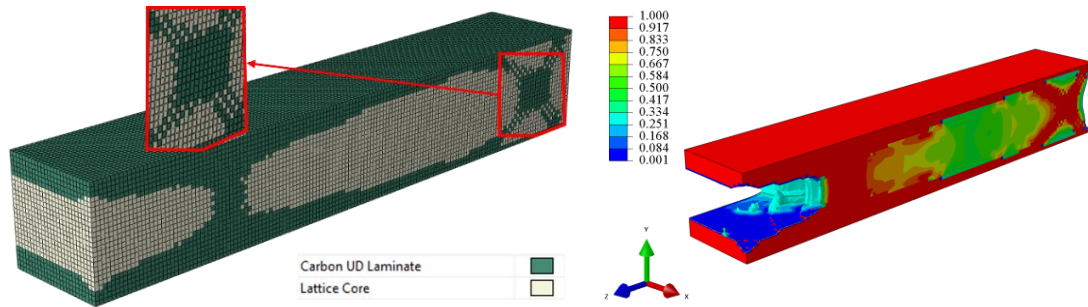


Figure 15: a) Breakdown of applied section properties for second stage optimisation with laminate sized using a relative density threshold value of 0.25 b) Second stage design for threshold of 0.25.

At a threshold value of 0.25, the solution is no longer feasible. This is shown in Figure 15, where small oscillations in the density across the domain introduce a checkerboard pattern of laminate elements, which are then used to great effect by the model to reduce mass, despite being unmanufacturable.

For this idealised design case, there is a large feasible region of designs, allowing for variation of laminate use to tailor for cost and manufacturability. This design process demonstration shows promise in the sizing of composite laminates with standard layups. In this longer beam configuration, without imposing a shear web laminate into the design, a foam core would not have been able to maintain the required stiffness of the beam to meet the displacement constraints. The shear modulus is too low in traditional core materials to prevent high shear deformations. In this case, ROHACELL[®] HERO 200 foam would only have been able to reduce shear deflection to 4.8 mm, over double the displacement constraint. Given the initial discrepancy between lattice design and performance in the short beam study, there is a possibility that the lattice core cannot achieve this displacement constraint either.

4 CONCLUSION AND AIMS OF FUTURE WORK

An initial benchmark study into the design capabilities of a novel methodology for hybrid composite-graded-lattice structures has been conducted. The design of each of the components in hybrid assembly was explored individually, by exploiting geometry to target different loading types and studying the features of topology optimisation solutions. In the first instance, a short beam with constant thickness composite skins was designed for a three-point-bend loading case, to investigate the compression and shear loading performance of an optimised graded lattice, while the skins reduced the bending load in the lattice. For the second instance, a longer beam underwent a two-stage optimisation to study the effect of varying the parameters used in the composite laminate sizing process. Together the results of these two studies set a baseline performance of this design method upon which improvements can be made.

The first study on the short beam found that, although it is possible to design graded lattice support structure, the displacement did not match the optimised density field. Through process-of-elimination this was found to be a result of the choice of penalisation factor in the topology optimisation and the unit cell size being too large to capture the optimised density field geometry. The effect of varying input parameters for the topology optimisation should therefore be studied in more detail so as to identify the best choice of penalisation factor, filter radius and mesh size. Another factor identified was the mismatch between the ‘real-life’ forces from a four point bending test and the boundary condition approximation used, which led to an increased error when using larger unit cell sizes.

The second study on the longer beam indicated that the laminate sizing process was successful in enabling the design of a hybrid composite-graded-lattice structure. It is possible to vary the amount of composite laminate to balance mass and cost of the design by varying a density threshold value in the first design stage. Limitations within this design process were identified on the lower end of the density threshold value scale as unmanufacturable features were allowed to be included through to the second stage of design. As the short beam study indicated poor agreement between optimised density field and graded lattice structural performance, the longer beam study will need to be conducted again with updated input parameters to confirm that this configuration is superior to conventional sandwich panels.

ACKNOWLEDGEMENTS

This project is funded by the Engineering & Physical Sciences Research Council, UK (CDT Grant Number: EP/S021728/1). The authors would also like to thank the Wind Blades Research Hub (WBRH), a collaboration between the University of Bristol and ORE Catapult, for their support of this work. This research is made possible by the software development of IDEA Lab on LatTess.

REFERENCES

1. T. D. Ngo, A. Kashani, G. Imbalzano, K. T. Q. Nguyen, & D. Hui, Additive manufacturing (3D printing): A review of materials, methods, applications and challenges. *Composites Part B: Engineering*, **143** (2018) 172–196. <https://doi.org/10.1016/j.compositesb.2018.02.012>.
2. SLM Solutions, MONOLITHIC THRUST CHAMBER. (2019).
3. M. Helou & S. Kara, Design, analysis and manufacturing of lattice structures: An overview. *International Journal of Computer Integrated Manufacturing*, **31** (2018) 243–261. <https://doi.org/10.1080/0951192X.2017.1407456>.
4. W. Jiang, G. Yin, L. Xie, & M. Yin, Multifunctional 3D lattice metamaterials for vibration mitigation and energy absorption. *International Journal of Mechanical Sciences*, **233** (2022) 107678. <https://doi.org/10.1016/j.ijmecsci.2022.107678>.
5. A. Panesar, M. Abdi, D. Hickman, & I. Ashcroft, Strategies for functionally graded lattice structures derived using topology optimisation for Additive Manufacturing. *Additive Manufacturing*, **19** (2018) 81–94. <https://doi.org/10.1016/j.addma.2017.11.008>.
6. J. Plocher & A. Panesar, Mechanical Performance of Additively Manufactured Fiber-Reinforced Functionally Graded Lattices. *JOM*, (2019). <https://doi.org/10.1007/s11837-019-03961-3>.
7. Martin Philip Bendsoe & Noboru Kikuchi, Generating optimal topologies in structural design using a homogenization method. *Computer Methods in Applied Mechanics and Engineering*, **71** (1988) 197–224.
8. O. T. Thomsen, Sandwich Materials for Wind Turbine Blades — Present and Future. *Journal of Sandwich Structures & Materials*, **11** (2009) 7–26. <https://doi.org/10.1177/1099636208099710>.
9. A. Moss, T. Macquart, A. Panesar, M. Forrest, P. Greaves, & A. Pirrera, Structural Design of Wind Turbine Blades with an Additively Manufactured Graded Lattice Core using Topology Optimisation. *Journal of Physics: Conference Series*, **2265** (2022) 032004. <https://doi.org/10.1088/1742-6596/2265/3/032004>.
10. G. Rozvany, The SIMP method in topology optimization - Theoretical background, advantages and new applications. *8th Symposium on Multidisciplinary Analysis and Optimization* (Reston, Virginia: American Institute of Aeronautics and Astronautics, 2000). <https://doi.org/10.2514/6.2000-4738>.
11. Y. Gandhi & G. Minak, A Review on Topology Optimization Strategies for Additively Manufactured Continuous Fiber-Reinforced Composite Structures. *Applied Sciences*, **12** (2022) 11211. <https://doi.org/10.3390/app122111211>.
12. K. W. Gan, S. R. Hallett, & M. R. Wisnom, Measurement and modelling of interlaminar shear strength enhancement under moderate through-thickness compression. *Composites Part A: Applied Science and Manufacturing*, **49** (2013) 18–25. <https://doi.org/10.1016/j.compositesa.2013.02.004>.
13. Simulia, Abaqus. (2022).
14. A. Panesar, LatTess. (n.d.).